Methods to Detect Habitable Atmospheres on the
Terrestrial Exoplanet TRAPPIST-1 e

by

D. Gatlin

Bachelor of Arts – Department of Astrophysical & Planetary Sciences

Undergraduate Honors Thesis

Defense Copy

Thesis Defense Committee:

Eric T. Wolf	Advisor	Atmospheric and Oceanic Sciences
Prof. Ann-Marie Madigan	Honors Council Representative	Astrophysical and Planetary Sciences
Prof. David Brain	External Faculty Member	Astrophysical and Planetary Sciences
Prof. Daniel Jones	External Faculty Member	Arts and Sciences Honors Program

To defend on:

2019–05–04

This thesis entitled:
Methods to Detect Habitable Atmospheres on the Terrestrial Exoplanet TRAPPIST-1 e
written by D. Gatlin
has been approved for the Department of Astrophysical and Planetary Science

_____

Dr. Eric T. Wolf

_____

Prof. Ann-Marie Madigan

_____

Prof. David Brain

_____

Prof. Daniel Jones

Date _____

The final copy of this thesis has been examined by the signatories, and we find that both the
content and the form meet acceptable presentation standards of scholarly work in the above
mentioned discipline.

Gatlin, D. (B.A., Astrophysics)

Methods to Detect Habitable Atmospheres on the Terrestrial Exoplanet TRAPPIST-1 e

Thesis directed by Dr. Eric T. Wolf

In order to better direct future exoplanetary research, we must be able to accurately predict what telescopes like the James Webb Space Telescope will be able to detect. To this effect, NASA's Planetary Spectrum Generator (PSG) can be used to simulate observations, both during exoplanet transits and at any time during an exoplanet's year. Such predictions allow us to make decisions about how to spend time on JWST and which techniques will allow for different types of science. In order to produce the most realistic results from the Planetary Spectrum Generator, self-consistent three-dimensional climate models of planets in the TRAPPIST-1 system are first used to simulate atmospheres on these tidally locked exoplanets, and understand how they might be different from the climate of Earth.

The TRAPPIST-1 exoplanets are assumed to be tidally locked with the host star. Recent climate modeling studies ~~conducted by Eric Wolf and others~~ indicate that there are three distinct types of tidally locked exoplanet atmospheres; slow rotators, fast rotators, and an intermediate regime. Slow rotators have large substellar clouds that remain constant over time. Fast rotators will have a significant Coriolis force, causing them to have much smaller substellar clouds and more intense zonal winds which advect clouds to the eastern side of the substellar point. In all three cases, the thermal emission of a planet depends strongly on the cloud ~~shape~~, which would change from the perspective of a distant observer over the exoplanet's year.

I have constructed a data pipeline that takes ~~Eric Wolf's~~ climate models as inputs, then sends them to the PSG to produce spectra. This pipeline can use a number of climate models on a number of different planets and can be used to create transit spectra or thermal phase curves.

When studying terrestrial exoplanets, the most exiting cases are habitable planets. The TRAPPIST-1 system is currently ~~the most likely~~ system to host a habitable exoplanet ~~because~~

~~of the variety of planets it hosts,~~ ~~and~~ TRAPPIST-1 e is the most likely habitable planet in the system. The most effective methods for JWST are the transit method and thermal phase curves. The transit method is the most popular method for detecting exoplanets, and JWST will have high resolution spectrographs that will be able to detect many atmospheric species including CO_2 and H_2O. Additionally, accurate spectra may enable us to infer information regarding the partial pressure of CO_2 remotely.

Transit spectra can tell us a lot about the terminator profile of an atmosphere, but it cannot tell us about other parts of the planet's surface. Transit spectra can also be prone to obscuration by clouds or aerosols. Thermal phase curves will observe the exoplanet over the course of its year, and may be able to detect features like the nature of the substellar cloud ~~and may be able to detect~~ if a planet has entered a runaway greenhouse effect or a snowball state. Thermal phase curves will look dramatically different for fast rotators like TRAPPIST-1 e compared to slow rotators, and these results can only be simulated with global circulation models used in conjunction with ~~line-by-line~~ radiative transfer models. Future predictions for JWST should incorporate global circulation models ~~into their predictions~~, and those models should be accurate to the exoplanets in question. Astronomers should also investigate thermal phase curves because they will be able to detect completely different features than transit spectra and will enable us to more effectively understand potentially habitable terrestrial exoplanets.

Dedication

To my Grandpa, Dr. Terry Flanagan

1938 – 2018

Acknowledgements

Thank you to all my family who helped encourage me on my way to becoming an astrophysicist. To my dad, my mom, and my sister. To my girlfriend, Grace Marshall.

Thank you to all my advisors I've had over my undergraduate career. To Susan (Astromom) Armstrong and David Brain. To Jeremy Darling and Seth Hornstein. To my research advisors Guy Stringfellow and Eric Wolf.

Thank you to everyone who read my drafts. To Donald Wilkerson and all my peers in PHYS 3050.

Thank you to my professors Zach Berta-Thompson, Nick Schneider, John Bally, Mathis Habich, Melissa Nigro, Jen Kay, Peter Pilewskie, and Alexandra Jahn. To my high school math teacher Laurie Buchanan.

Thank you to my co-investigators Eric Wolf, Ravi Kopparapu, Geronimo Villanueva, and Avi Mandell.

Facilities: Exoplanet Archive, Planetary Spectrum Generator

Contents

Chapter

Tables

Table

Figures

Figure

Chapter 1

Introduction

Exoplanetary science is one of the most exciting fields in astrophysics, despite barely existing 20 years ago. Until the Kepler mission, it was ~~thought that exoplanets were rare~~, but we have since estimated that approximately one third of all F, G, and K stars have at least one terrestrial exoplanet (Traub, 2012). ~~A majority of discovered exoplanets are large gas giants that orbit extremely close to their host star, so called "Hot Jupiters." Although these planets are exotic and revolutionary for planetary formation theories, they cannot possibly support life due to the lack of a surface and their extreme temperatures~~. ~~More~~ excitingly, we have found a number of terrestrial exoplanets which resemble Earth in mass, size, and most crucially, solar irradiance. These terrestrial exoplanets are the most likely candidates in the search for habitable worlds beyond Earth, and by extension, our most likely places to discover extraterrestrial life or a future home for humanity. To date, the list of exoplanets in the classical habitable zone is short, and few are close to Earth, but this will soon change with the recently launched Transiting Exoplanet Survey Satellite (TESS). TESS is expected discover thousands of exoplanets smaller than Neptune and dozens of Earth sized planets, and was optimized for finding planets that are closer to Earth (Ricker et al., 2014). In conjunction with the James Webb Space Telescope (JWST), we expect to dramatically improve our observations of potentially habitable worlds in nearby star systems.

Exoplanets are likely tidally locked due to their close orbit to their host star (Turbet et al., 2018), meaning they don't rotate relative to their star. Our solar system contains no example of such a planet. Tidally locked planets behave ~~so~~ differently from ~~any atmosphere in our solar system~~,

that the only way to characterize their atmospheres is via global circulation models (GCMs). GCMs were invented for purposes like predicting the weather or climate change, and have proven useful for a number of different planets throughout the solar system (Way et al., 2018). Many astronomers have made predictions of what JWST will see on exoplanets, but most of these predictions assume that an exoplanet atmosphere can be similar to that of Earth (Fortney et al., 2018). However, recent 3D climate modeling experiments demonstrate that exoplanets are very different than Earth. For example, an exoplanet that receives approximately the same amount of sunlight as Earth, TRAPPIST-1 d, is less likely to be habitable than TRAPPIST-1 e, a planet that receives only 60% of the solar irradiance of Earth (Wolf, 2018).

With the launch of JWST on the horizon, it is essential that we know what to expect from our observations with it, and atmospheric models are our best method of putting constraints on our expectations. Simply assuming a tidally locked exoplanet will behave like Earth is unreasonable and can lead to inaccurate conclusions. Using GCMs for TRAPPIST-1 d, e, and f provided by Dr. Eric Wolf, we can self-consistently predict what the TRAPPIST-1 exoplanets may look like with regards to clouds features, distributions, precipitation, and temperature. NASA's Planetary Spectrum Generator (PSG) can generate spectra for these climate models, giving us accurate predictions of what JWST might be able to see (Villanueva et al., 2018). Using the PSG, we can determine which spectral features would be detectable with JWST and using signal to noise analysis, we will help the astrophysics community prioritize their time with JWST.

In addition to exoplanet spectra, GCMs allow us to study exoplanets using other methods, most notably thermal emission phase curves. A GCM provides global resolution of an exoplanet's surface and atmosphere, but only a small fraction of it is visible via the transit method. The PSG can allow us to measure the thermal emission of the surface of the planet as it rotates relative to the Earth over its year. Thermal phase curves measure the change in thermal brightness of an exoplanet as it orbits its star, and can be variable over time in a way that could be detected with JWST. Thermal phase curves have the advantage of strong signal to noise due to large binning and long observation times. This technique serves as our best method of resolving features like clouds

on exoplanets, and by extension, the planet's climate. Thermal phase curves and transit spectra provide two very unique methods of probing an exoplanet's atmosphere, and together, they will help JWST find habitable worlds beyond Earth.

In this thesis, I will calculate both transit spectra and thermal phase curves several exoplanets, particularly TRAPPIST-1 e. In the following section, Chapter 2, I will explain the fundamentals of exoplanet research and exoplanet observations, with an emphasis on the variables significant to thermal phase curves and transits. In Chapter 3, I will interpret climate models from Wolf (2018), and particularly focus on the terminator atmosphere profile and the global cloud patterns. I will compare fast rotators and slow rotators, which have dramatically different cloud patterns, and therefore different thermal phase curves. In Chapter **??**, I will explain the data pipeline used and the PSG as a tool to simulate spectra. In Chapter **??**, I will show transit spectra results, analyze their behavior, and identify and measure prominent features. In Chapter **??**, I will do the equivalent analysis for thermal phase curves, and compare slow rotators versus fast rotators here. In Chapter **??**, I will conduct a noise analysis, and compare the signal to noise ratios of transits and thermal phase curves.

Chapter 2

Background

Isaac Newton was the first person to consider the possibility of exoplanets (Newton, 1846). It requires little more than a simple understanding of the solar system and Newtonian physics to consider the possibility that other stars may host their own planets. Any planet orbiting any star must obey Newton's version of Kepler's 3rd law,

$$T^2 = \frac{4\pi^2}{G\left(m_* + m_p\right)}a^3,$$ (2.1)

where T is the orbital period of the orbit, a is its semi-major axis, m_* is the mass of the star, and m_p is the mass of the planet. In addition, the small mass approximation where $m_* >> m_p$ simplifies equation 2.1 to

$$T^2 = \frac{4\pi^2}{Gm_*}a^3,$$ (2.2)

which we can solve, even if the mass of the planet is unknown. If the orbital period of an exoplanet and the mass of the host star are known; the planet's semi-major axis can be calculated. Using the semi-major axis, the planet's solar irradiance can be calculated with

$$S_p = \sigma T_*^4 \frac{r_*^2}{a^2},$$ (2.3)

where S_p is the solar irradiance for the exoplanet. This value can be calculated using only a few data points, and can be compared to the solar irradiance of Earth ($S_\oplus \approx 1361\mathrm{W\,m^{-2}}$). A simple narrative would be that if the $S_p \approx S_\oplus$, then the planet is Earth-like. This understanding defined exoplanetary knowledge for hundreds of years, and very little progress was made for a long time because of observational limitations.

The most naïve method for detecting an exoplanet is by directly imaging them, just like we do for stars; however, the math behind this isn't very promising. If you approximate a planet as a blackbody, its flux is proportional to R^2T^4, then a 300K exoplanet with a radius of $1R_\oplus$ around a 3000K star with a radius of $0.17R_\odot$ would be $1/10,000,000^{\text{th}}$ as bright, which corresponds to a difference in 16 magnitudes. While observing two stars 16 magnitudes apart is certainly possible in optimal circumstances, it is virtually impossible to do in the case of exoplanets because an exoplanet and its host star are almost always within the diffraction limit of each other. Telescopes large enough to detect an exoplanet have existed for over a hundred years, but the primary limitation has always been the instrumentation. A photometric plate could never have detected an exoplanet.

This changed with the introduction of a type of digital camera called a CCD, where accurate photometry of dim objects can be done in minutes, not hours. Astronomers were now able to detect exoplanets with a new method, not by measuring the brightness of the planet, but by measuring the change in the brightness of the star. In 2003, the first exoplanet was detected by measuring the decrease in the star's brightness as the planet passed in front of its host star (Konacki et al., 2003). This became known as the "transit method," and to date, this method has detected more exoplanets than any other. The transit method only requires simple photometry, which can be done with significantly higher signal to noise than spectroscopy. Transits are usually found using relative photometry, meaning the brightness of a star during transit is compared to the brightness of other stars in the field. This means that measurements can be accurate despite the presence of systematic errors. In a transit, the measured signal is the decrease in the brightness of the star relative to its normal brightness, so the measured value is called transit depth, and can be given by

$$D = \frac{R_p^2}{R_*^2}, \tag{2.4}$$

where D is the transit depth, R_p is the planet radius, and R_* is the star radius. Using the above example of a $1R_\oplus$ planet around a $0.17R_\odot$ star, the transit depth would be 0.0028, or $3/1000^{th}$ the brightness of the star, which can be measured fairly reliably. The most observable exoplanets are

large planets around small stars. Small stars are less likely to drown out the signal of a planet, and large planets are likely to create larger signals. A large planet around a small star would have a large transit depth. It is worth noting that transit depth is usually reported in parts per million (ppm) instead of as a decimal, as it will for the remainder of this thesis.

Another useful exoplanet detection method is the radial velocity method. As an exoplanet orbits its host star, the star should move as well much more slowly than a planet. With the use of a spectrograph, the doppler shift of a host star can be measured. Usually a star may be moving at speeds so low, they're measures in centimeters per second, but it can still be measured reliably. By applying the laws of conservation of momentum, the relationship

$$m_* v_* = m_p v_p, \tag{2.5}$$

where m represents the mass, v represents the velocity, * represents the star and p represents the planet. The star mass is known from the star's temperature and size, and the planet's velocity can be deduced from Kepler's laws. This method can be useful for measuring the masses of large planets, but the radial velocity methods fails when the planetary mass is too small to produce a large stellar velocity. This method was able to find an exoplanet over 10 years before the first transit (Latham et al., 1989). The radial velocity method can often be used in conjunction with the transit method because transiting exoplanets will produce the strongest possible radial velocity measurements. For more complicated systems with multiple planets, the radial velocity method becomes more difficult, and other methods are more useful for measuring planetary mass.

Other exoplanet detection methods have developed, such as gravitational lensing and astrometry. However, all of these methods are fairly limited in both efficiency and scope.

Unfortunately, there are some major limitations to the transit method. The most exciting exoplanets are terrestrial exoplanets are approximately $1R_\oplus$, approximately $1m_\oplus$, and have approximately $1S_\oplus$. For these planets in particular, the transit method has proven to be the most effective method. For large stars, smaller planet become impossible to detect as their transit depth is too small. With even the best scopes, it can take years to measure terrestial exoplanets around

sun-like stars. The Earth-Sun system has a transit depth of 84ppm, which is orders of magnitude smaller than the average transit. A planet very similar to the Earth-Sun system called Kepler-452b has been found (Jenkins et al., 2015), but a recent study by Mullally et al. (2018) has argued that the system doesn't have strong enough signal to noise to be confirmed as an exoplanet. Another major limitation is that only a small number of exoplanets orbit in an observable plane. If we assume that an exoplanet can orbit in any random plane relative to Earth, and we can only detect it if its orbital plane is within 3°, then $\sim 3\%$ of exoplanets can be detected from Earth. In reality, the actual cutoff of an "in plane" exoplanet is more complicated and depends on a number of other variables, but 3°is a good first-order estimate. Our ability to detect smaller transit depths will improve over time, but the inclination issue is an inherent limitation to the transit method. Only transiting exoplanets will be considered for the remainder of this thesis. It is worth noting that the conclusions made with transiting exoplanets can be easily generalized for non-transiting exoplanets because there is nothing unique about a transiting system other than its relation to Earth.

For transiting exoplanets, there are a few coordinate conventions that must be described explicitly. Firstly, there was the previously mentioned issue of the coordinate plane in which a planet rotates. The angular difference between the orbital plane and Earth is called the *inclination*, denoted here by θ. A visual example of inclination is given in Figure 2.1. There is also the position of the exoplanet in its orbit, which is called *orbital phase*. Conventionally, the phase where an exoplanet is perfectly behind its host star is set to 0°(an occultation, or sometimes a type-II transit), and the phase where an exoplanet is perfectly in the middle of a transit is set to 180°(also called a type-I transit). A visual explanation of phase is given in Figure 2.2. Surprisingly, it doesn't matter which direction the exoplanet orbits in as long as the convention is consistent. In this paper, the orbital phase will be called ϕ and will be to the left for $0° \leq \phi \leq 180°$ and to the right for $180° \leq \phi \leq 360°$

As has already been alluded to, a majority of exoplanets are found around small stars, mostly K-type and M-type stars, due to observational biases that favor detections in these systems. These stars are far redder than Sun-like stars, and emit far less light. This means that in order for

a planet to receive similar TSI to Earth, it must be much closer to its parent star. Exoplanets found in the habitable zones of late-K and M-dwarf stars are likely to be tidally locked, meaning that they rotate synchronously with their parent star. The Moon is tidally locked to the Earth, which is why we always see the same face of the Moon, but it still rotates relative to the Sun. With exoplanets that are tidally locked relative to their parent stars, one half of the planet will get constant sunlight, and another side of the planet will never receive Sunlight. In this situation, a new set of useful terminology can be used to describe constant points on the planet's surface. The point that is always facing the Sun is the substellar point. The point that is opposite to the substellar point is the antistellar point. The line that is equidistant from the substellar and antistellar point is called the terminator. The substellar point is equivalent to Earth at noon, when the sun is directly overhead; the antistellar point is equivalent to the Earth at midnight; and the terminator is equivalent to the Earth at Sunset and Sunrise.

Any point on a spherical object can be defined using two angles, and the most standard convention is latitude (δ) and longitude (λ), where the equator is defined as $\delta = 0°$, the North Pole is $\delta = 90°$, and the South pole is $\delta = -90°$. Longitude ranges from 0 to 360, and on Earth, the "zero point" is completely arbitrary. In the case of tidally locked planets, we set the zero point to be conveniently aligned with the antistellar point, so the substellar point is at ($\lambda = 180°, \delta = 0°$).

Of all the exoplanets discovered, the TRAPPIST-1 system provides the most interesting case in the search for habitable exoplanets, and will therefore be a primary target for the upcoming JWST mission. Around the star TRAPPIST-1, there are 7 exoplanets, named alphabetically from b to h. They are all roughly $1m_{\oplus}$ and $1R_{\oplus}$. TRAPPIST-1 is a very cool M-dwarf with a temperature of 2511K, at a distance of 12pc from Earth (Delrez et al., 2018). TRAPPIST-1 b has a TSI of $3.8S_{\oplus}$, which is by any measure, too hot for anything even remotely close to life. TRAPPIST-1 h on the other end has a TSI of $0.13S_{\oplus}$, which must be far too cold to support life. Since both ends of the spectrum are covered, it's reasonable to hope that somewhere in the middle, one or two of the remaining 5 are similar enough to Earth to support life.

Using the work done by Turbet et al. (2018), it is reasonable to conclude that all the

TRAPPIST-1 planets are tidally locked and have an eccentricity low enough to approximate it as 0. With the known parameters of the TRAPPIST-1 system found by Gillon et al. (2017), the next logical step is to run climate models to more accurately estimate habitability.
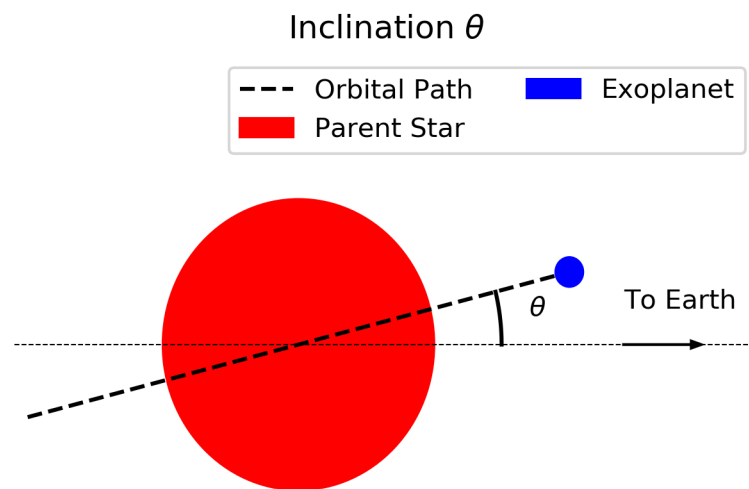
Figure 2.1: Simple depiction of inclination. Any possible exoplanet can be viewed from this angle, making inclination a universal tool for characterizing exoplanets. Typically, an exoplanet with an inclination of less than 3° can have a transit, although this isn't the most rigorous definition, and the actual value depends on planet size and star size. However, the closer to 90°, the better because that means longer transits and therefore better measurements.
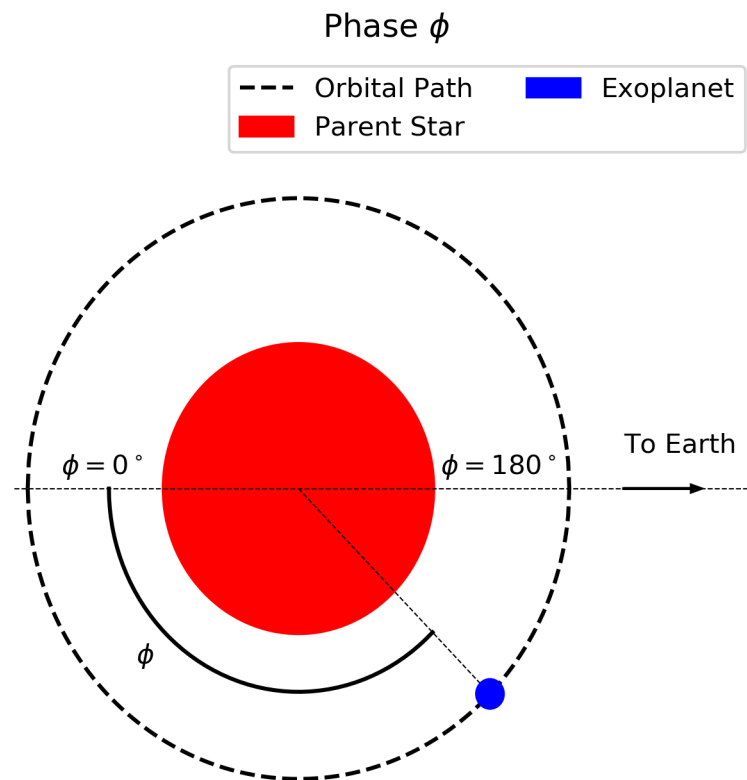
Figure 2.2: Simple depiction of phase. In this diagram viewing from above, phase first goes down, then up. The convention of phase can be defined relative to transits and occultations, and regardless of the direction of this convention, the math behind which latitudes face Earth remain constant.
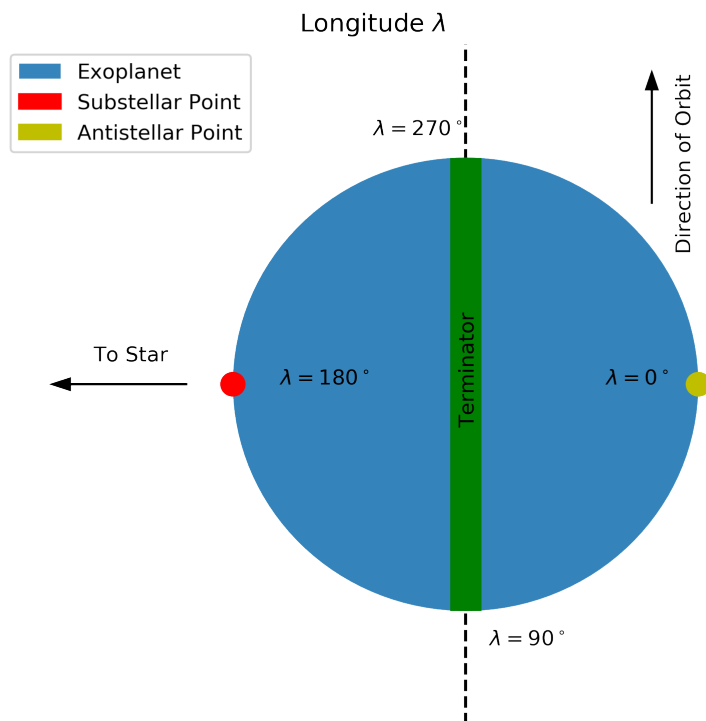
Figure 2.3: Simple depiction of longitude for a tidally locked planet. These longitudes are correct for any phase or inclination. Note that from Earth during a transit $\lambda = 0°$ when $\phi = 180°$, and they move in opposite directions.

Chapter 3

Climate and Atmosphere Models

In this study, I use the 3D climate modeling simulations of Wolf (2018) as a starting point for analysis of spectral signals that may be detected with JWST and other telescopes. Therefore, it is important to review the results of ~~Eric Wolf's~~ climate models in order to adequately understand any conclusions derived from them. Many of the conclusions discussed here will have significant impacts on later sections. Transit spectra is sensitive to the atmospheric composition, and in order to characterize that sensitivity, many climate models with varying parameters must be tested. For thermal phase curves, clouds are particularly important. Climate models allow us to predict the distribution of clouds on the TRAPPIST-1 planets, giving us insight into what we would see from a thermal phase curve. Cloud distributions depend on the availability of water vapor, the temperature of the planet, and on the large scale atmospheric circulation, which itself depends on the strength of the Coriolis force, which is determined by the rotational rate of the exoplanet. Assuming that the TRAPPIST-1 exoplanets are tidally locked allows us to set their rotation rate to their orbital period, allowing us to precisely constrain the influence o the Coriolis force.

Climate models have proven to be a very useful tool to accurately predict behavior of an atmosphere. A climate model uses fundamental physics like radiative transfer, convection, the Coriolis force, and other rules to predict the motion of air parcels iteratively through time. One popular climate model is the Community Atmosphere Model 4 (CAM4), provided by the National Center for Atmospheric Research (Neale et al., 2012). Using a modified version of CAM4, Wolf (2018) was able to apply climate models to the tidally locked exoplanet of the TRAPPIST-1 system

including TRAPPIST-1 d, TRAPPIST-1 e, and TRAPPIST-1 f. All of the climate models for TRAPPIST-1 d entered a runaway greenhouse, even in models without CO_2. All of the models for TRAPPIST-1 f ~~were extremely cold, even with extreme amounts of CO_2,~~ TRAPPIST-1 e had ~~several~~ models which were ~~very~~ habitable, making TRAPPIST-1 e is the most promising candidate of the system for supporting habitable conditions. Although other cases will be considered, this paper will focus primarily on TRAPPIST-1 e.

Climate models can be used to determine the impacts of a variety of species in the atmosphere. In these models, fixed amounts of CO_2 and N_2 were given, while H_2O is allowed to ~~varry~~ self-consistently by CAM4. CO_2 will always tend to warm an atmosphere. This tendency is because of the greenhouse effect, and only molecules with 3 or more atoms will contribute to the greenhouse effect directly because they contain vibrational modes which can store energy levels that correspond to infrared wavelengths. 2-atom molecules like N_2 cannot contain vibrational modes, and thus cannot absorb or emit infrared light. However, adding N_2 to an atmospheric model will increase the pressure, which can impact the absorption of infrared light by CO_2. Unlike atomic emission features, which absorb and emit at discrete wavelengths, molecular emission features are broad, and although they peak at a fixed wavelength, they will emit or absorb light for a large range of wavelengths around the peak wavelength. Increasing the pressure of a greenhouse gas has the tendency to broaden this emission feature, and therefore increase its efficacy as a greenhouse gas. For this reason, adding N_2 to an atmosphere can also increase the atmosphere's average temperature. H_2O, like CO_2, is a greenhouse gas and exhibits pressure-broadening behavior. More importantly, H_2O is not well mixed in an atmosphere, and may condense in the atmosphere as liquid clouds, ice clouds, or vapor, as well as condense on the surface as ice, snow, or water. The primary advantage of running a 3D climate model is to allow for self-consistent calculations of water in its various phase, as distributed across a planet by general circulation.

A number of climate models have been run, and recently, Wolf has included CH_4, which is a stronger greenhouse gas than CO_2 or H_2O. All of the climate models are shown in Table 3.1. Of this list, many of the models for TRAPPIST-1 e have global mean temperatures that appear

too low or too high to support life. The Earth's mean atmospheric temperature is ~300K (Wang et al., 2005), and some of the models are able to get similar temperatures. From this list, the most interesting models are the $1barN_2$, $0.2barCO_2$, and $1barN_2$, $0.4barCO_2$ because they have a global mean temperature closest to that of modern day Earth, although some others also stand out as strong candidates for habitability.

Despite what Table 3.1 and Figure 3.1 suggest, habitability can be very complicated to define. Most of the details about habitability are questions of biology. Many finer details about how life would look on TRAPPIST-1 e cannot be inferred from these models. All of these models use a global ocean but ignore ocean currents, which is a major method of heat transport. None of the models include land masses, which would change both ocean currents and atmospheric currents. Many significant atmospheric species like O_2, O_3, N_2O, and others aren't included, despite their obvious significance in Earth's atmosphere. CO_2 abundance is set as a model parameter, but in reality, its abundance would be driven by geologic processes over timescales much longer than where CAM4 would be useful. Some geologic models of exoplanets have found that negative feedbacks between CO_2 and H_2O will tend to cause the partial pressure of CO_2 to converge to a habitable value with liquid water (Kite & Ford, 2018).

In addition to climate models, many equations useful for Earth's atmosphere can help us describe the TRAPPIST-1 system. Anthropogenic climate change on Earth was predicted by Dr. Svante Arrhenius, who created an effective equation to predict the warming of an atmosphere, given an increase in CO_2. Arrhenius' rule is given as

$$T = \alpha \ln \left(\frac{C}{C_0} \right) + T_0 \tag{3.1}$$

where C is the current amount of CO_2 in the atmosphere, C_0 is the former amount of CO_2 in the atmosphere at a given time, and T_0 is the global atmospheric temperature at that time, α is a constant that depends on a number of things not considered in this model. For TRAPPIST-1 e, this equation can be very useful. In Figure 3.1, it can produce a reliable best fit line. A similar fit can be made for increasing N_2, and is shown in Figure 3.2.

N_2	CO_2	CH_4	H_2	Surface Temperature
bar	bar	bar	bar	K
0	0.25	0	0	237.7
0	0.5	0	0	268.0
0	1	0	0	303.0
0	2	0	0	333.2
0.9	0	0	0.1	229.2
1	0	0	0	217.4
1	0.0004	0	0	234.2
1	0.0004	1.7×10^{-6}	0	236.1
1	0.01	0	0	248.1
1	0.1	0	0	270.2
1	0.2	0	0	281.5
1	0.4	0	0	301.0
1	1	0	0	330.2
1.5	0.1	0	0	280.9
1.5	0.2	0	0	294.9
2	0.1	0	0	286.7
2	0.2	0	0	306.1
4	0.1	0	0	319.0
4	0.2	0	0	332.2
10	0.2	0	0	358.4

Table 3.1: TRAPPIST-1 e Models and Species Abundances. Each row represents a single climate model of TRAPPIST-1 e, with each column showing the amount of a given species in that model. The surface temperatures are an average of the 3 longitudes closest to the terminator.
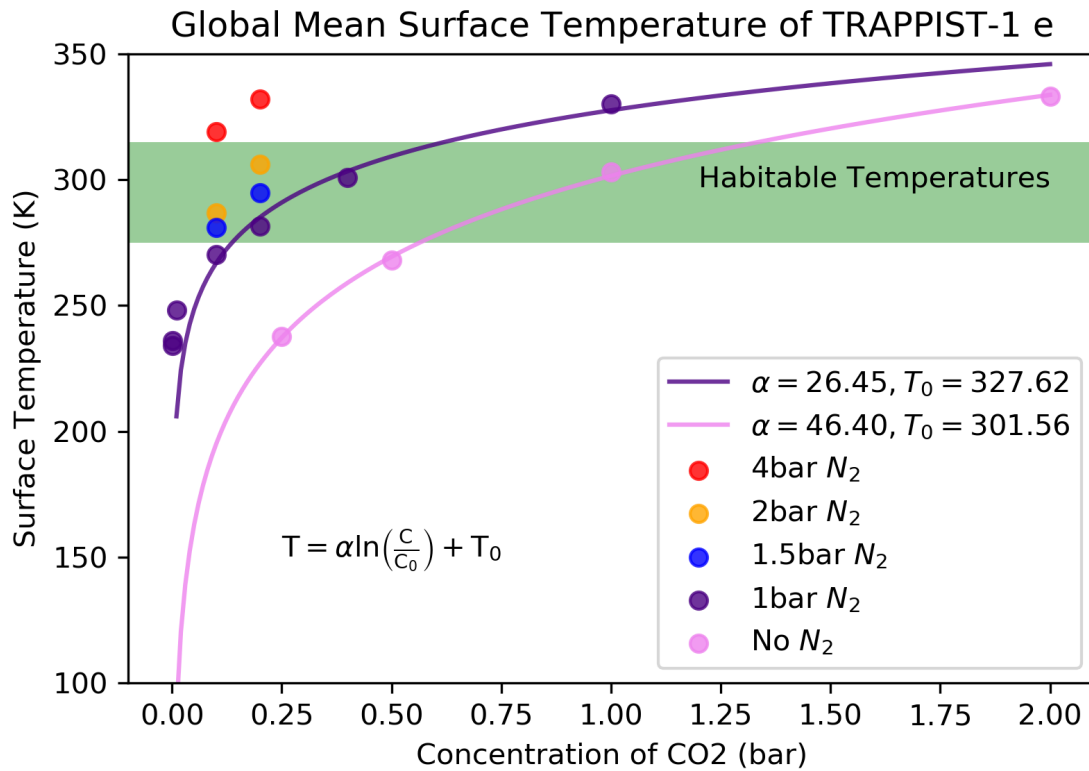
Figure 3.1: ~~Terminator~~ surface temperature versus CO_2 partial pressure. Most of the models in Table 3.1 are shown here to more accurately demonstrate the relationship between CO_2 and warming. Both CO_2 and N_2 can contribute significantly to the warming of the planet, but they do so differently because N_2 is not a greenhouse gas. In this diagram, the "habitable zone" is between 275K and 315K, following the definition by Wolf et al. (2017). It is just a general estimate of where the most likely habitable worlds would likely be.
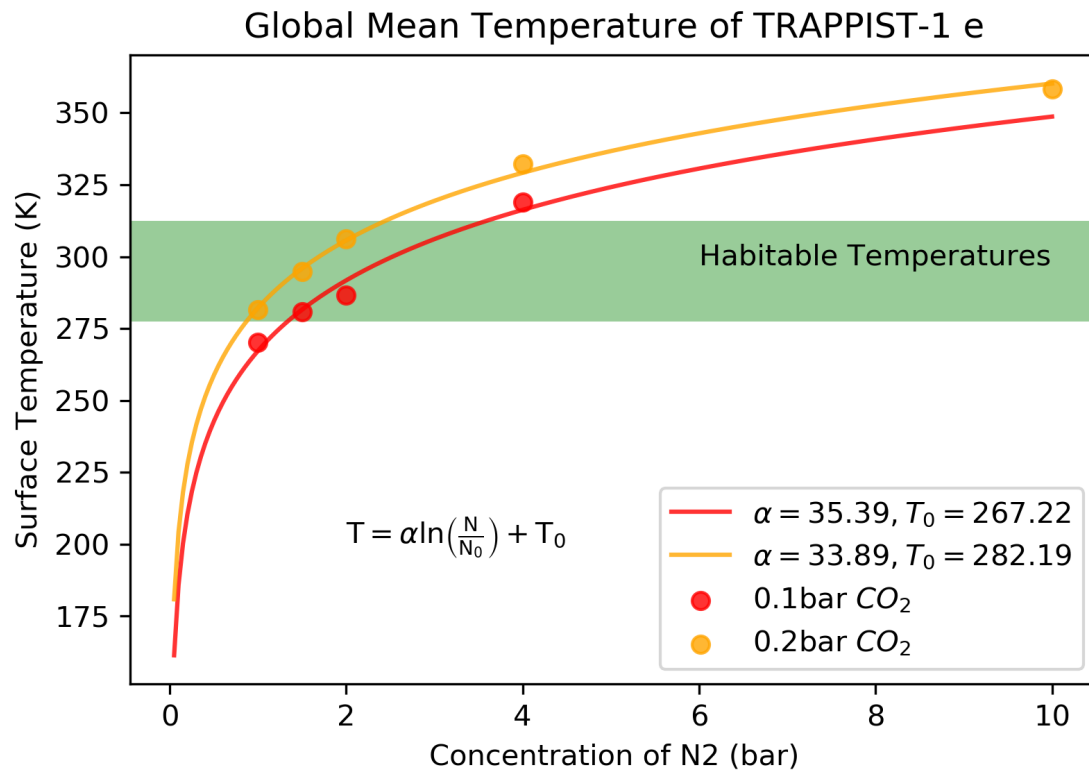
Figure 3.2: ~~Terminator~~ surface temperature versus N_2 partial pressure. Similarly to Figure 3.1, logarithmic best fit lines match the data well, although the fit is noticably better for CO_2 than N_2.

~~So far, I have only examined the mean temperature of the terminator.~~ For the purposes of transits, ~~this~~ is the only significant section of the atmosphere, but for thermal phase curves, spatial resolution is a necessity, largely due to the presence of a substellar cloud (Kopparapu et al., 2017). CAM4 models the atmosphere using a discrete number of points, making a 3D array of coordinates where there are 72 longitudinal bins, 46 latitudinal bins, and 40 vertical bins. Each attribute of a model like temperature, cloud amount, etc. all have their own data cubes. In order to display the data, it must be reduced from a 3D set. A useful method of displaying data like cloud abundance is using a column density. Each vertical layer of the atmosphere has a different cloud abundance, but we're mostly concerned with the total cloud abundance, which would be the sum of all the different layers. This more closely represents what the clouds would look like from a distant observer. Figures 3.3 and 3.5 are both column densities of liquid cloud abundance and precipitation.

A major influence on the structure of clouds in an atmosphere is the Coriolis force. The acceleration due to the Coriolis force is given as $a_C = 2\mathbf{v} \times \mathbf{\Omega}$, where $\mathbf{v}$ is the velocity of a particle and $\mathbf{\Omega}$ is the rotational frequency of the planet. Earth has a rotational frequency of $2\pi/24$hr, so the Coriolis force plays a major role in atmospheric physics. TRAPPIST-1 e has no rotation relative to the Sun, but because its year is only 6 days (Gillon et al., 2017), it will have an angular frequency of $2\pi/6$d, which is significantly less than Earth's, but still strong enough to drive significant zonal circulation. The effects of TRAPPIST-1 e's Coriolis force can be clearly seen in Figure 3.3. The substellar cloud is fairly small, and is concentrated to the east, while the ~~western~~ substellar point has little to no clouds.

Kopparapu et al. (2017) has run models on other synchronously rotating exoplanets, including some idealized exoplanets with set parameters such as solar irradiance and orbital period. These models can easily be put into two categories, fast rotators and slow rotators. An extended orbital period means that the Coriolis force is much weaker, which produces a completely different shape for its substellar cloud. The substellar hemisphere is covered by clouds, and the substellar cloud is fairly symmetric from the east to west and north to south. According to Haqq-Misra et al.

(2018), fast rotators have a period of less than 5 days, slow rotators have a period of greater than 20 days, and the region in between is called the Rhines rotation regime. ~~To a remote observer, Rhines rotators and fast rotators are extremely similar, but their characteristic difference is that a Rhines rotator has stronger circullation.~~ TRAPPIST-1 e is on the boundary between the two, exhibits characteristics of both. For the purposes of this investigation, the most important feature is a relatively contained substellar cloud, shown in Figure 3.3. Slow rotators (like the 44 day one shown in Figure 3.4 have large substellar clouds that are highly symmetric and cover most of the planet's day side.

In addition to surface features, one of the most useful tools to describe a planetary atmosphere is its profile. During an exoplanet transit, light will pass through the atmosphere, and the lower atmosphere will be too opaque, and little light will make it through, but the upper atmosphere will be much less dense, allowing more light through. This means that atmospheric features that are close to the planet's surface would be much harder or impossible to detect compared to upper atmosphere features. According to Figure 3.6, a majority of the clouds are concentrated in the lower atmosphere, meaning that H_2O will be harder to see in an exoplanet transit than CO_2 which is well mixed at all levels of the atmosphere. From Figure 3.6, a thermal inversion close to the surface can also be seen, meaning that the temperature goes up with height for a brief period. This has the effect of stabilizing the atmosphere and on Earth, can cause pollution to be trapped near the surface (Fortelli et al., 2016). In this plot, the effective temperature is given, which is what the temperature of the planet's surface would be if it had no atmosphere, and is given by the equation

$$T_e = \sqrt[4]{\frac{S(1-\alpha)}{4\sigma}} \tag{3.2}$$

where T_e is the equilibrium temperature, S is the solar irradiance, α is the albedo, and σ is the Stefan-Boltzmann constant. The shape of an atmosphere's profile is significant for a

While these models are extremely illustrative of many details about the TRAPPIST-1 e atmosphere, there are a number of noteworthy assumptions that limit our predictive capabilities. These models don't include O_2, which is a vital element for living organisms. Adding O_2 would
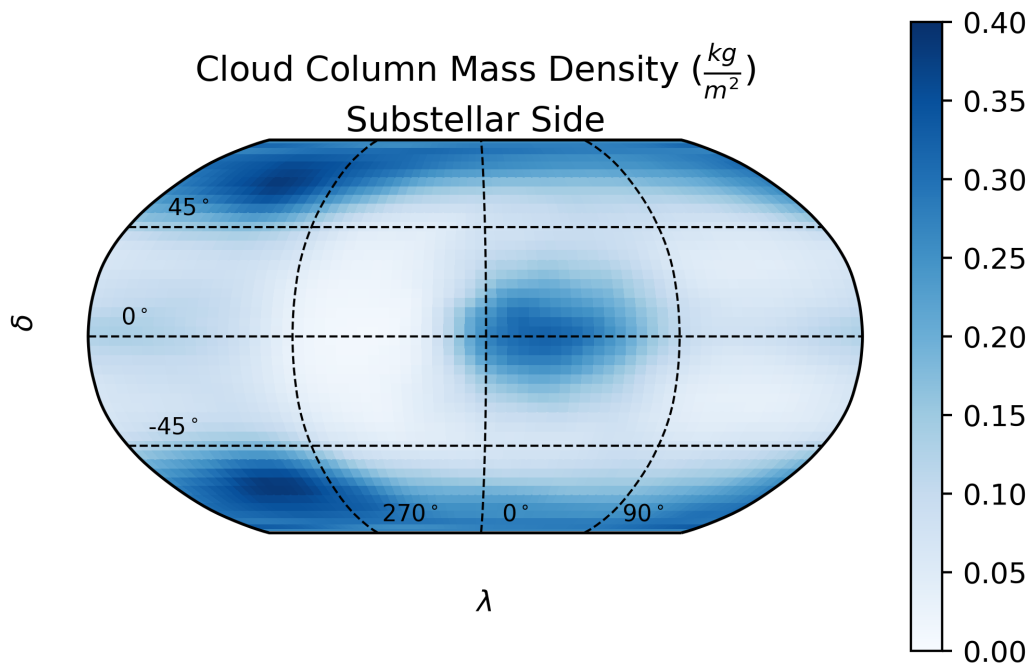
Figure 3.3: Cloud Column Density of TRAPPIST-1 e with 1bar N_2 0.4bar CO_2. In this image, white represents very dense clouds, and blue represents few to no clouds. For the substellar point, there are strong clouds, particularly on the eastern side. Surprisingly, right next to the substellar point is also the region with the least amount of clouds. This is due to the planet's rotation, which causes a Coriolis force that produces asymetric substellar clouds. ~~In CAM4, clouds are measured as mass densities of the cloud particle mass in each grid point divided by the total mass inside that grid point, which is where the units of $\frac{kg}{kg}$ come from. When summing the column, the units don't change.~~
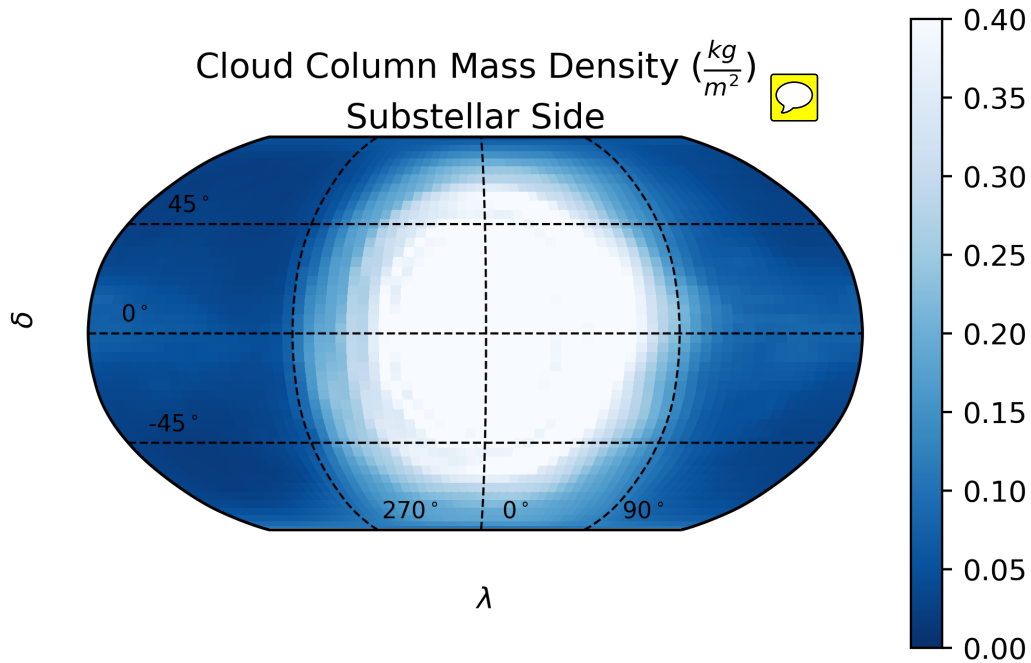
Figure 3.4: Cloud Column density of a slow rotator. The planet used here is a slow rotator with an orbital period of 44 days. In this case, it received significantly more solar energy from TRAPPIST-1 e, which will cause it to be extremely warm and therefore have much stronger clouds than TRAPPIST-1 e. The absolute scaling of the cloud amount is less important than the shape of the clouds. Here, the clouds are extremely symmetrical and large. This is a dramatic difference from the behavior of the TRAPPIST-1 e model in Figure 3.3.
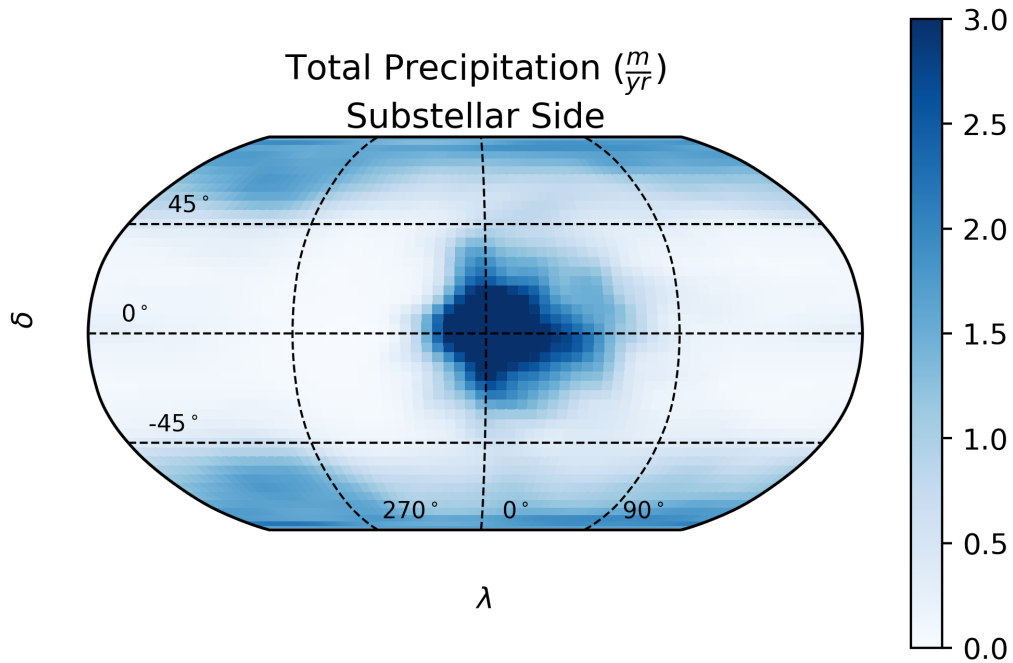
Figure 3.5: Precipitation of TRAPPIST-1 e with 1bar N_2 0.4bar CO_2. In this image, blue represents high amounts of precipitation and white represents little to no precipitation. From Figure 3.3, we can conclude there is a persistent substellar cloud, but in order to determine if there's actually rain reaching the surface, one must also check its precipitation since the presence of clouds doesn't always mean there must be rain. There does appear to be very localized substellar rain indicated by the blue dot, but the rest of the planet only has marginal amounts of rain in comparison.
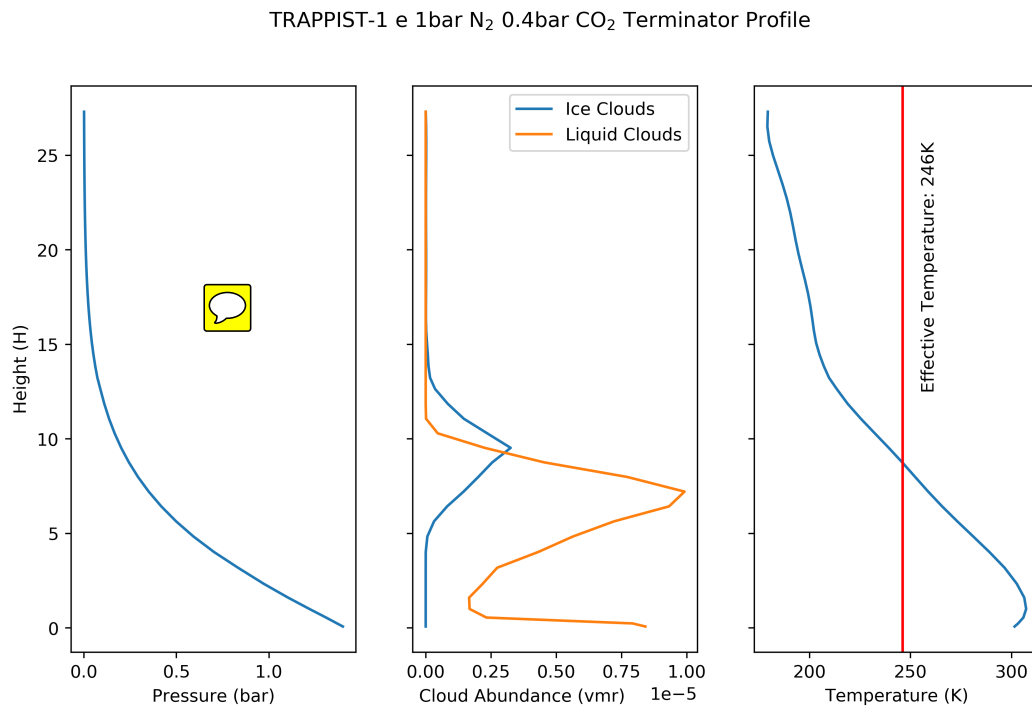
Figure 3.6: Profile of TRAPPIST-1 e with 1bar N_2 0.4bar CO_2.

dramatically complicate the models because it would require a prognostic chemistry calculation, which would imply the addition of O_3 as well, a greenhouse gas and the primary species in the stratosphere. These TRAPPIST-1 e models do not include a stratosphere, which would be a second thermal inversion higher up in the atmosphere. These models are long term models run over 40 years, and they only have enough resolution to determine general features. Unlike a weather forecast model; these models cannot accurately predict small weather features in the TRAPPIST-1 e atmosphere, the models are only useful for general, long-term trends. These climate models do not include any trace atmospheric species, most notably N_2O, but there are many more species that could be detected during a transit from a telescope.

Chapter 4

Methods

The James Webb Space Telescope is set to launch some time in 2021, and it will cost over \$8.7 billion five years after launch. With such an expensive project, we need to be able to accurately predict how it will operate before it launches to determine what how we should spend our time on it. Villanueva et al. (2018) have created the Planetary Spectrum Generator (PSG) specifically with this in mind, and can simulate a variety of planetary observations using a variety of telescopes. The PSG's most important feature is its line by line radiative transfer model (PUMAS), which depends strongly on the given atmosphere profile. The climate models discussed in chapter 3 provide a useful input to the PSG, but the climate models are very complex and they must first be adapted into formats supported by the PSG. The bulk of the work for this thesis was creating a data pipeline to make climate models compatible with the PSG. In this chapter we will discuss the techniques used to convert the models from Wolf (2018) into inputs for the PSG and how the PSG uses those inputs to produce spectra.

Climate models have many outputs. Attributes like temperature, species abundance, pressure, and many more are stored in latitude x longitude x altitude array. Other parameters like surface temperature, albedo, and surface pressure are stored in latitude x longitude arrays. Other parameters have only one planetwide value like gravity and orbital period. Climate models output a complex filetype that stores all these values, but only a few of them are relevent for the PSG. Additionally, some values are not included in the climate model like the distance between the star and the observer, the orbital inclination, and many more. These parameters aren't atmospherically

important, but they're very important astrophysically, so they are needed by the PSG.

Additional parameters that were not given my the climate model were found using NASA's exoplanet archive. The parameters used from the exoplanet archive were name, mass, radius, diameter, semi-major axis, inclination, transit depth, insolation, star radius, star velocity, star effective temperature, star distance, star magnitude, star metallicity, and star logarithmic surface gravity.

The PSG only takes an atmospheric profile, so the 3D climate model data had to be reduced down. How this should be done depends on the type of measurement taken. For an exoplanet transit, the significant part of the atmoshere is the terminator profile because that is where light from the star will pass through the atmosphere and towards the observer. For all other phases, the most significant part of the atmosphere is the Earth facing side.

For the transit case, the phase is $180°$, which means the left hand side has a phase of $270°$ and the right hand side has a phase of $90°$. In most cases for the models in Wolf (2018), these phases correspond to exactly a single grid cell, but in order to generalize the project code, the average of all cells that fit the criteria of $\lambda = 270° \pm 5°$ **or** $\lambda = 90° \pm 5°$. This method would work even if there was no longitude corresponding exactly to $\lambda = 270°$ **or** $\lambda = 90°$.

For a transit, all longitudes and latitudes are weighted equally because the grid cells are spaced evenly across latitudes. In order to compute a transit profile, the points are averaged with equal weighting according to the equation

$$\mathrm{x}_i\left(\phi\right) = \frac{\int_{85,265°}^{95,275°} \int_{-90°}^{90°} \mathrm{x}_{i,\delta,\lambda}\, \mathrm{d}\delta \mathrm{d}\lambda}{\int_{85,265°}^{95,275°} \int_{-90°}^{90°} \mathrm{d}\delta \mathrm{d}\lambda}, \tag{4.1}$$

where x is a parameter at a grid cell of height i, latitude δ, and longitude λ. Latitude and longitude are averaged, but the heights are not, so Equation 4.1 would reduce a 3D climate model to a 1 dimensional profile for each parameter x. The parameter x can be used to represent temperature, pressure, or volume mixing ratio of any of the tracked species.

For the non-transit case, many variables that were fixed in the transit case are no longer

constant. Inherent to a latitude-longitude grid is the convergence of points near the poles. The result is that each grid cell occupies less area near the poles, and should therefore be weighted less in the average by a factor of $\cos(\delta)$. In addition, the Earth facing side contributes more to the emission towards Earth than the limbs. The result of this is a second factor of $\cos(\delta)$ to account for the latitudinal component and a factor of $\cos(\lambda + \phi)$ to account for the longitudinal component. The resulting value is a disk average given by the equation

$$\mathrm{x}_i\left(\phi\right) = \frac{\int_{-\phi-90°}^{-\phi+90°} \int_{-90°}^{90°} \cos^2(\delta) \cos(\lambda + \phi) \mathrm{x}_{i,\delta,\lambda}(\phi) \, \mathrm{d}\delta \mathrm{d}\lambda}{\int_{0°}^{360°} \int_{-90°}^{90°} \cos^2(\delta) \cos(\lambda + \phi) \, \mathrm{d}\delta \mathrm{d}\lambda}, \tag{4.2}$$

which is the same as Equation 4.1, except for the addition of a weighting in the cosine of λ and δ, and a dependence on ϕ. Physically, this equation can be described as taking a 3D sphere of the planet and simplifying it to a 2D projection as seen from the observer, then averaging the observed value (Cowan & Agol, 2008; Koll & Abbot, 2015). This method means that any atmospheric parameter x that varies with respect to ϕ should change relative to the observer. The cosine squared for latitude indicates that there is a strong preference for latitude, and atmospheric features that are significantly north or south of the equator should only weakly contribute to the disk averaged value.

This disk weighted average explicitly shows the weighting function used, but implicitly in the integrals, there is also a mask, where only half of the planet is used in the calculation at any given time. This is because only half of the planet is facing Earth, and the other half therefore shouldn't contribute to the average. If the limits were to include the anti-Earth facing side, it would include negative values due to the cosine term, which would be nonsensical. In Figure 4.1, these two behaviors are shown side by side.

For the transitting case, a different masking scheme is used, and no weighting scheme is used. A similar diagram to Figure 4.1 is given for the transit case in Figure 4.2.

The whole purpose of averaging these values is that the 3D climate model can be reduced to an atmosphere profile that can be put into the PSG. The parameters used from the climate model

profile were height, pressure, temperature, and the volume mixing ratios of N_2, CO_2, CH_4,H_2O, liquid clouds, ice clouds, liquid cloud size, ice cloud size. Additionally, surface pressure, surface temperature, surface albedo, and dry molecular weight were used, but they do not varry with height, so they are not part of the profile.

In an exoplanet transit, light will pass through the atmosphere and be collected by a telescope. A majority of an exoplanet's atmosphere is far too thick for light to enter one side and make out the other. As light passes through any medium that could absorb it, it should be extinguished according to Beer's Law

$$\frac{I}{I_0} = \exp(-n\sigma L), \tag{4.3}$$

where I is the intensity of the light as seen by the observer, I_0 is the intensity of the light at the source, n is the particle number density, σ is the cross-sectional area of the particles, and L is the length of the path that light travels. In an exoplanet transit at low altitudes, n is far too large, so I/I_0 is too small to be detected. σ and L don't varry much across an atmosphere, but n will decrease as a function of height, approximately exponentially as given by the equation

$$\frac{n}{n_0} = exp(\frac{-z}{H}) \tag{4.4} \qquad\qquad H = \frac{k_B T}{mg} \tag{4.5}$$

where z is the height, n is the density, k_B is the Boltzmann constant, T is the atmospheric temperature, m is the average molecular weight, and g is the gravitational force. This means the upper atmosphere will be much less dense than the lower atmosphere. The CAM4 climate models only have grid point to pressures as low as 1mb, which is low enough for most atmospheric physics. However, for transit spectra, this is still relatively opaque, and n must be decreased even more for significant amounts of light to pass through the atmosphere. To amend the atmosphere models for the purposes of tranist spectra, additional layers must be added to the atmosphere. These layers must also have pressure drop off exponentially. Temperature decreases with height at those levels, but this effect is igored, and all the added layers have a constant temperature given by the top

layer of the climate model. Additionally, the ratios of all atmospheric species are kept the same as the top layer of ~~hte~~ climate model.

For the purposes of the PSG, only a few layers were necessary because the PUMAS ratiative transfer model includes a very accurate sub-layering scheme. For all simulations used in this project, 7 layers were added, and the top layer was at a pressure of 10^{-6}mb. Pressures this low are well beyond the necessary range and guarantee that the PSG will have atmospheric inputs capable of simulating an exoplanet tranist.

The PSG can ~~be operated a number of ways~~, the most fundemental of which are W/m^2 and raw counts, which represent what a telescope would actually see. The PSG can also return an already reduced output that simply shows the transit depth. This reduced method can be derived from either raw method, but is more convenient for analysis, and is therefore the most commonly used. The PSG can produce a tranist spectra, as well as the components that make it up including the solar emission and the planet's thermal emission, although it's worth noting that neither of those are actual observables of an exoplanetary system. In an actual exoplanet observation, only the raw total signal can be observed.

The results from the PSG separate the noise from the signal, although that's not how it would actually be observed. Signals without noise allow us to make predictions about observations, and noise can be used later to determine how long it would take to make conclusions about those observations. There are other noise simulators for James Webb that rival that of the PSG, and often could use the PSG's spectra as an input. For this reason, the PSG only needs to be run once to get results on the signal, and the exposure time doesn't impact those results. Exposure time would only affect the signal-to-noise ratio.

For transits, the PSG needs to be run only once ~~because the signal will never change~~. For thermal phase curves, ~~the signal itself will change,~~ so the PSG must be run multiple times to compute a thermal phase curve. Thermal phase curves should ~~varry~~ continuously, and so one might assume that they could compute thermal phase curves with arbitrary resolution, but this isn't possible using 3D climate models because the averaged atmosphere profile won't change unless

ϕ varries by more than 5°because that is the longitudinal resolution of the climate models. If you examine Figure 4.1 closely, you can in fact see the grid cells in the climate model. This means that in order to compute thermal phase curves with higher resolution than 5°, it would require higher resolution climate models. However, the point is moot, TRAPPIST-1 e has an orbital period of 6.01days (Gillon et al., 2017), and therefore orbits at a rate of $\sim 2.5° hr^{-1}$. In an actual observation of a thermal phase curve, it's reasonable to be observing for multiple hours, so a climate model with 72 longitudinal bins will have similar or greater resolution in ϕ than the maximum possible resolution from observations in ideal conditions.
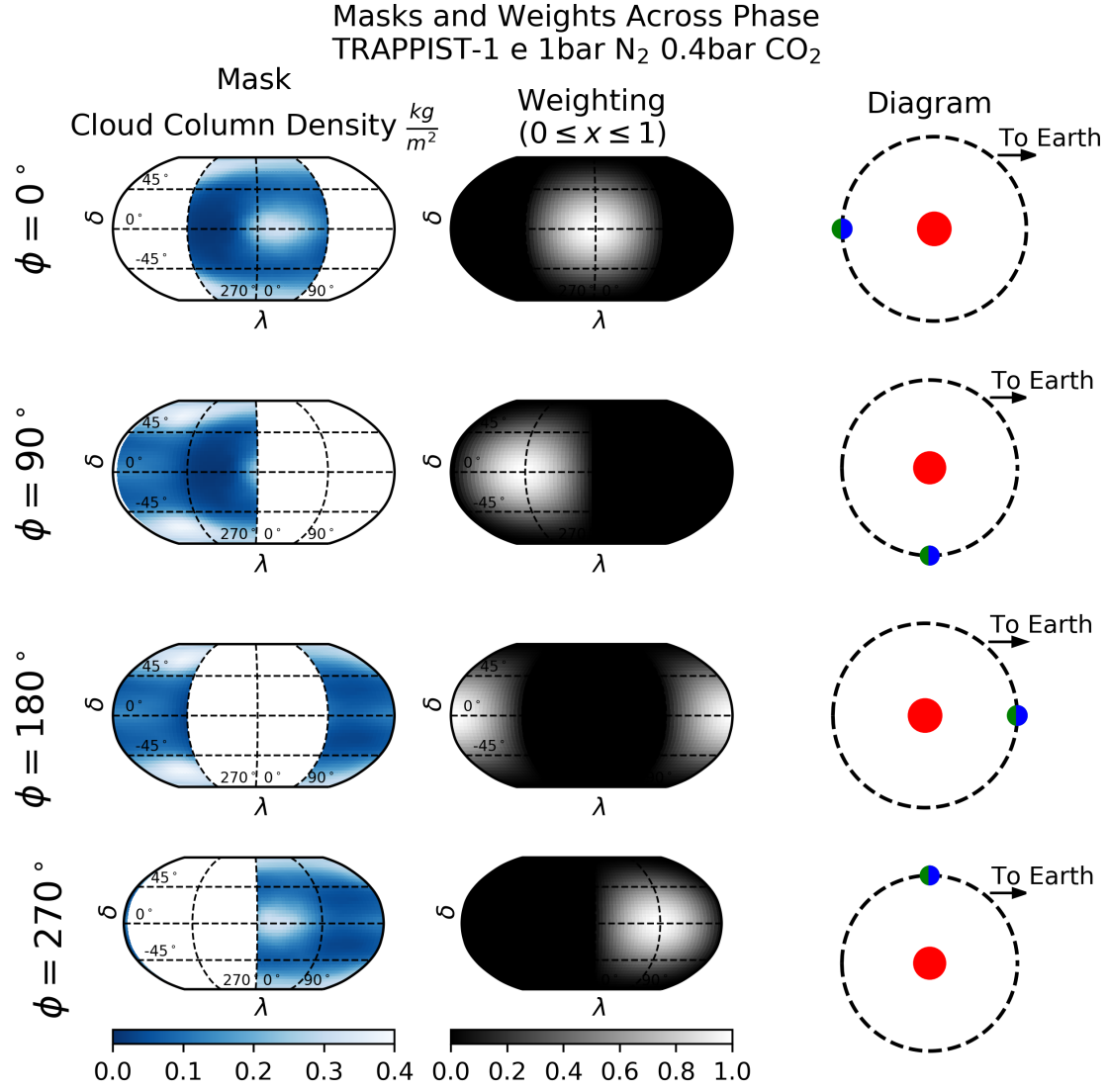
Figure 4.1: Surface masks and weights across phase. As a planet rotates through *phi*, the Earth facing side of the planet will change. The climate model used in the mask diagram is the TRAPPIST-1 e 1bar N_2 0.4bar CO_2 case. At different points through the year, the substellar cloud will move in and out of view. Parameters like emissivity should decrease as the cloud is in view and increase when the western side without clouds are in view.
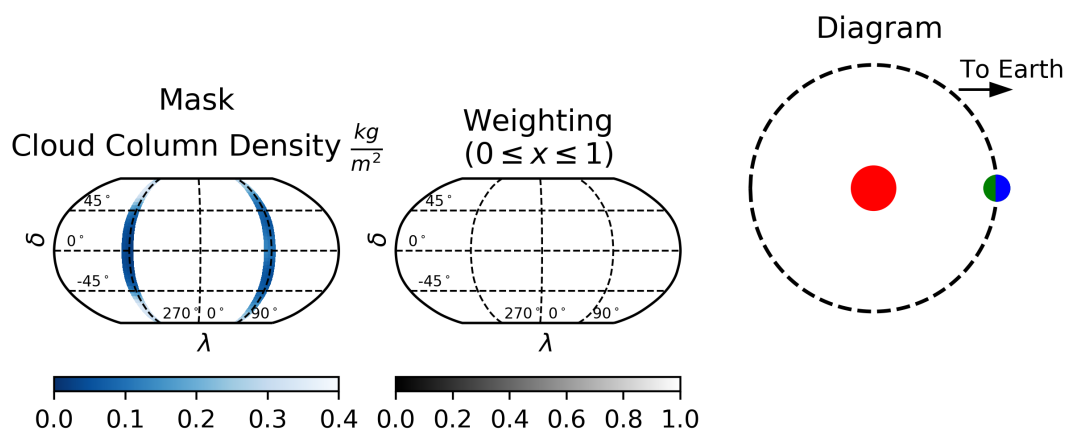
Figure 4.2: Surface masks and weights for transits. For the tranissing case, a weighting function is unnecessary, but it is included for consistency with Figure 4.1. The more significant detail is that the masking scheme is discontinuous with the disk averaged values over the remainder of the exoplanet's year.

References

2018, James Webb Space Telescope, Tech. rep., Goddard Space Flight Center

2019, NASA Exoplanet Archive, https://exoplanetarchive.ipac.caltech.edu/

Cowan, N. B., & Agol, E. 2008, ApJL, 678, L129, doi: 10.1086/588553

Delrez, L., Gillon, M., Triaud, A. H. M. J., et al. 2018, MNRAS, 475, 3577, doi: 10.1093/mnras/sty051

E Walter, M. 2010, Notices ofthe maerican Mathematical Society, 57

Fortelli, A., Scafetta, N., & Mazzarella, A. 2016, Atmospheric Environment, 143, 218 , doi: https://doi.org/10.1016/j.atmosenv.2016.08.050

Fortney, J., Kataria, T., Stevenson, K., et al. 2018, arXiv e-prints, arXiv:1803.07730. https://arxiv.org/abs/1803.07730

Gillon, M., Triaud, A. H. M. J., Demory, B.-O., et al. 2017, Nature, 542, 456, doi: 10.1038/nature21360

Haqq-Misra, J., Wolf, E. T., Joshi, M., Zhang, X., & Kopparapu, R. K. 2018, ApJ, 852, 67, doi: 10.3847/1538-4357/aa9f1f

Jenkins, J. M., Twicken, J. D., Batalha, N. M., et al. 2015, AJ, 150, 56, doi: 10.1088/0004-6256/150/2/56

Kite, E. S., & Ford, E. B. 2018, The Astrophysical Journal, 864, 75

Koll, D. D. B., & Abbot, D. S. 2015, The Astrophysical Journal, 802, 21

Konacki, M., Torres, G., Jha, S., & Sasselov, D. D. 2003, Nature, 421, 507

Kopparapu, R. k., Wolf, E. T., Arney, G., et al. 2017, ApJ, 845, 5, doi: 10.3847/1538-4357/aa7cf9

Latham, D. W., Mazeh, T., Stefanik, R. P., Mayor, M., & Burki, G. 1989, Nature, 339, 38, doi: 10.1038/339038a0

Leconte, J., Wu, H., Menou, K., & Murray, N. 2015, Science, 347, 632, doi: 10.1126/science.1258686

Mullally, F., Thompson, S. E., Coughlin, J. L., Burke, C. J., & Rowe, J. F. 2018, AJ, 155, 210, doi: 10.3847/1538-3881/aabae3

Neale, R. B., Chen, C., & Gettelman, A. 2012

Newton, S. I. 1846, Mathematical Principles of Natural Philosophy

Ricker, G. R., Winn, J. N., Vanderspek, R., et al. 2014, 9143, 914320, doi: 10.1117/12.2063489

Traub, W. A. 2012, The Astrophysical Journal, 745, 20

Turbet, M., Bolmont, E., Leconte, J., et al. 2018, A&A, 612, A86, doi: 10.1051/0004-6361/201731620

Villanueva, G. L., Smith, M. D., Protopapa, S., Faggi, S., & Mandell, A. M. 2018, JQSRT, 217, 86, doi: 10.1016/j.jqsrt.2018.05.023

Wang, J., Zhang, L., & Dai, A. 2005, Journal of Geophysical Research: Atmospheres, 110, doi: 10.1029/2005JD006215

Way, M. J., Del Genio, A., & Amundsen, D. S. 2018, arXiv e-prints, arXiv:1802.05434. https://arxiv.org/abs/1802.05434

Wolf, E. T. 2018, The Astrophysical Journal Letters, 855, L14

Wolf, E. T., Shields, A. L., Kopparapu, R. K., Haqq-Misra, J., & Toon, O. B. 2017, ApJ, 837, 107, doi: 10.3847/1538-4357/aa5ffc